Chemie der Erde 74 (2014) 353–363

Contents lists available at ScienceDirect

Chemie der Erde

journal homepage: www.elsevier.de/chemer

Historical mercury trends recorded in sediments from the Laguna del Plata, Córdoba, Argentina

Yohana Vanesa Stupar[a,b], Jörg Schäfer[c,d], María Gabriela García[b], Sabine Schmidt[c,d], Eduardo Piovano[b], Gérard Blanc[c,d], Frédéric Huneau[e,f], Philippe Le Coustumer[a,*]

[a] Université de Bordeaux, EA 4592 Géoressources & Environnement, ENSEGID, 1 allée F. Daguin, F-33607 Pessac, France
[b] Centro de Investigaciones en Ciencias de la Tierra (CICTERRA), CONICET/Universidad Nacional de Córdoba, Av. Vélez Sarsfield 1611, X5016CGA Córdoba, Argentina
[c] Université de Bordeaux, EPOC, UMR5805, F-33400 Talence, France
[d] CNRS, EPOC, UMR5805, F-33400 Talence, France
[e] Université de Corse Pascal Paoli, Laboratoire d'Hydrogéologie, Campus Grimaldi, BP 52, F-20250 Corte, France
[f] CNRS, UMR 6134 SPE, BP 52, F-20250 Corte, France

ARTICLE INFO

Article history:
Received 20 March 2013
Accepted 5 November 2013
Editorial handling - H. Guo

Keywords:
Mercury speciation
Selective extractions
Hydroclimatic variability
Laguna del Plata
Laguna Mar Chiquita
Evaporates
Córdoba
Argentina
Metal records in sediments

ABSTRACT

The main carrying phases of mercury (Hg) were analyzed in a 120 cm sediment core taken at the Laguna del Plata (LP), a small lake connected to the main water body of Laguna Mar Chiquita (LMC) during high-stands. LMC is considered to be one of the largest saline lakes in the world representing a sensitive climatic indicator due to its frequent lake level variations at millennial and interdecadal scale like the last ones that started early in the 1970s and after 2004. Total particulate Hg (Hg_{TP}) concentrations vary between ~13 and ~131 $\mu g\,kg^{-1}$ indicating a system with low pollution. Selective extractions with ascorbate, HCl and H_2O_2 were performed in the sediments and they revealed that Hg is associated mainly to reactive sulphides in the base of the core, while in the middle and upper part the organic matter seems to be the main Hg-bearing phase. The highest and most important peak was found in sediments accumulated between 1991 and 1995. More than a punctual source of pollution, this peak is likely related to two eruptive events occurred in the Andean Cordillera in this period: the eruption of Hudson volcano in southern Patagonia that occurred in 1991 and the one of the Láscar volcano in northern Chile that occurred in 1993. In both cases, the respective ash plumes were documented to have reached the Laguna del Plata region.
© 2013 Elsevier GmbH. All rights reserved.

1. Introduction

Mercury (Hg) is mobilized naturally through geological and volcanic activities (Fitzgerald and Lamborg, 2003) but due to human activities such as coal burning, industry and mining, the cycle of mercury has been altered increasing long-term particle transport in the atmosphere and making deposition three to five times larger than preindustrial deposition in the northern Hemisphere (Selin, 2009). This element can be transported in the atmosphere in three forms: as elemental gaseous mercury Hg(0), divalent mercury Hg(II) in small water droplets or particulate mercury Hg(P). Because divalent and particulate Hg are more soluble in water than elemental Hg, they are the Hg predominant forms deposited in the ecosystem through wet and dry deposition (Fitzgerald and Lamborg, 2003; Selin, 2009). Particulate Hg may account for more than 90% of total Hg in freshwater systems, estuaries or coastal zones (Fitzerald and Mason, 1997; Balcom et al., 2004; Schäfer et al., 2006) and sediments can represent efficient Hg traps and archives of past contamination (Gagnon et al., 1997; Castelle et al., 2007).

In countries such as Canada, France, Switzerland and China, the highest Hg concentrations are observed at the beginning of the 19th Century due to the demographic and industrial growth such as "the golden age" (1860), or the Second World War (1939–1945) among others. These events were responsible for the release and accumulation of this metal in sediments, and even with the implementation of clean technologies and more strict environmental laws, concentrations are 2–3 folds higher than preindustrial times (i.e. Von Guten et al., 1997; Johannessen et al., 2005; Castelle et al., 2007). In South America, most of the high Hg concentrations are linked to gold mining in countries such as Colombia, Bolivia and Peru where high Hg levels were found in river and lake sediments, soils, fishes and human hairs in (Olivero et al., 2002; Rodrigues Bastos et al., 2006). Hg is used for separation of gold particles through amalgamation. During this process, a good amount of metallic Hg is also lost to rivers and soils through handling under rough field conditions and to volatilization. After amalgamation, the Au–Hg complex

* Corresponding author. Tel.: +33 620310431.
E-mail address: plc@lnet.fr (P. Le Coustumer).

0009-2819/$ – see front matter © 2013 Elsevier GmbH. All rights reserved.
http://dx.doi.org/10.1016/j.chemer.2013.11.002

is burned in retorts but in most areas, this operation is done in open air, releasing Hg vapour to the atmosphere. Furthermore, Hg rich tailings are left in most mining sites (Diaz, 2000; Lacerda et al., 2004). In the southernmost part of the continent, where pristine conditions are still conserved, Hg concentrations measured in sediments accumulated in lakes during the last century were attributed to volcanic events, soil erosion and the influence of global Hg fluxes (Ribeiro Guevara et al., 2010; Hermanns and Biester, 2013).

In Argentina in particular, the occurrence of Hg in sediments accumulated in freshwater systems are scarce (i.e. Amin et al., 1996; Hudson-Edwards et al., 2001; Ronco et al., 2001; Marcovecchio et al., 2001; Ribeiro Guevara et al., 2002, 2005, 2009, 2010; Arribére et al., 2003; De Marco et al., 2006; Botté et al., 2010). Most of these studies are concentrated in the Patagonia region and in coastal areas of the Buenos Aires province. For example, De Marco et al. (2006) analyzed total Hg concentrations in sediments and biota in three estuarine systems on the shores of Buenos Aires between the years 1980 and 2005. The results indicate that total Hg values decreased significantly ($p < 0.001$) in the last 25 years attributing this trend to the improvement in the industry practices. In the Argentina Patagonia, where the population density is low, Ribeiro Guevara et al. (2010) concluded that the high Hg concentrations measured in lake sediments of pre-industrial time are due to extended fire records and volcanic activity.

Even though aquatic ecosystems are globally exposed to Hg by atmospheric inputs of increasing concern, few studies have been focusing on the sources, fate and history of freshwater systems of the southern hemisphere (Downs et al., 1998; Lamborg et al., 2002; Biester et al., 2007). In this context, the study of Hg accumulation in the sedimentary record in Laguna del Plata (30°55′S, 62°51′W) is a contribution to understand the fluxes of global Hg in a climatic-sensitive region of southern South America (e.g. Piovano et al., 2004a,b).

Laguna del Plata (30°55′S, 62°51′W) is situated in the SW margin of the Laguna Mar Chiquita system, composed by the Laguna del Plata, linked to the main water body, the Laguna Mar Chiquita itself and the Dulce River wetlands. The area has a rich biodiversity as well paleontological and archaeological interest to the point that the lake has been declared as a Ramsar site by the United Nations (Bucher et al., 2006). Laguna del Plata is fed by the Suquía River (200 km length and average discharge of 10 $m^3 s^{-1}$) that reaches the lake from its southern margin. The river headwaters are located in the Sierras Pampeanas de Córdoba (between 29°00′–33°30′S and 64°00′–65°30′W) where different mining activities (mainly rock quarries) and land-use have been developed. The San Roque reservoir (643 m.a.s.l.) collects the waters from the catchment's tributaries and is used for flood control and drinking water reservoir. Downflow, the Suquía River crosses from West to East the city of Córdoba which is the second biggest of Argentina (1.3 million inhabitants) after Buenos Aires. Automobile industry, machinery manufacturing, food and paint production are the main economical activities in the city. In its lower stretch, the Suquía River crosses the loessic depression of the Chaco Pampean Plain (Zárate, 2003) which is one of the most important agricultural areas of the country. Some authors (Pesce and Wunderlin, 2000; Wunderlin et al., 2001; Monferrán et al., 2011; Pasquini et al., 2011) observed a decrease in the water quality from pristine regions in the upper fluvial catchments to the proximity of the lake. And even if Gaiero et al. (1997) noticed an increase in trace metal concentrations in riverbed sediments downflow attributed to the urban impact, Hg was not included into the studied ones. At present there is no comprehensive data on the long-term change in metal contents of the Suquía River sediment load.

The present study focuses on the sedimentary record of Hg concentrations and its main operationally-defined carrier phases in Laguna del Plata over the past ~80 years. Due to its already documented sensibility to global changes, climatic-driven variability of a typical atmospherically transported element such as Hg, will be clearly recorded in the sediments accumulated in this lake. In consequence, the main objective of this work is to understand if and how global change factors, such as population growth and/or hydroclimatic variability (lake-water level changes) affect lacustrine Hg concentrations and solid state speciation in this part of South America.

2. Materials and methods

2.1. Study area

2.1.1. Background

Laguna Mar Chiquita is the biggest saline lake in South America and one of the largest in the world conserving still a wild and little altered physiognomy (Bucher et al., 2006). Three rivers pour their waters into the lake (Fig. 1a): (i) The Suquía River; (ii) The Xanaes River (total length 340 km and average discharge of 14.5 $m^3 s^{-1}$); and (iii) The Dulce River (total length of 812 km and an average discharge of 80 $m^3 s^{-1}$), which is the biggest one, and has its catchments in the North-West region of Argentina.

During the 20th Century, Laguna Mar Chiquita showed important water-level and surface variations (Fig. 1b). The first 75 years of the 20th Century Laguna Mar Chiquita was characterized by low levels but in the decade of 1970s a wet spell started (Piovano et al., 2009) and high levels were registered. From 2003 to 2004 up to nowadays Mar Chiquita has been showing decreasing lake levels. Low and high water stands were defined as below or above 66.5 m.a.s.l. water altitude (average value) being synchronous with decreasing and increasing average regional precipitation (Piovano et al., 2002). During these stages, water salinities changed from 360 g L^{-1} in 1911 (Frank, 1915) to 270 g L^{-1} in 1970 (Martínez, 1991) and 35 g L^{-1} in 1989 (Martínez et al., 1994). Even in extreme dry periods with almost non-existent river supply, the lake was never completely desiccated due to groundwater recharge (Piovano et al., 2002, 2004a,b) but it was disconnected from Laguna del Plata until the early 1970s (see satellite images Fig. 1b). Accordingly, important differences existed between both systems, with lower water salinity in Laguna del Plata due to the diluting effect of Suquía River (Reati et al., 1997).

2.1.2. Climatic and geological settings

The Laguna Mar Chiquita system catchment covers an area of around 127,000 km^2, (between 62–66°W and 26–31°S). Austral summer precipitation and dry winters characterize the climate of the region, where the only external sources of water vapour for rainfall are the Atlantic Ocean and the tropical latitudes, which is related to the development of a monsoon-like climatic system (Garreaud et al., 2009). The ENSO (El Niño Southern Oscillation) teleconnections also control precipitation and the hydrology of major riverine systems (Aceituno, 1988; Depetris et al., 1996; Silvestri, 2004; Boulanger et al., 2005; Pasquini et al., 2006). Based on the studies of long cores (~3 m) retrieved from Laguna Mar Chiquita, interpretation of satellite images, drilled cores and fieldwork, Piovano et al. (2004a,b, 2009) determined the paleoenvironmental evolution of the area during the late Quaternary (last 13,000 years). The analyzed hydroclimatic record of Laguna Mar Chiquita indicates the onset of a positive hydrological balance at 13.0 cal ka BP (calibrated thousand years Before Present). This period was followed by extremely dry conditions that triggered the precipitation of evaporates and more positive isotope composition of carbonates and organic matter. After 6.8 cal ka BP there was an increase in the temperature gradient as a result of an enhanced influence of the Southeast Pacific anticyclone, larger Antarctic sea-ice extend

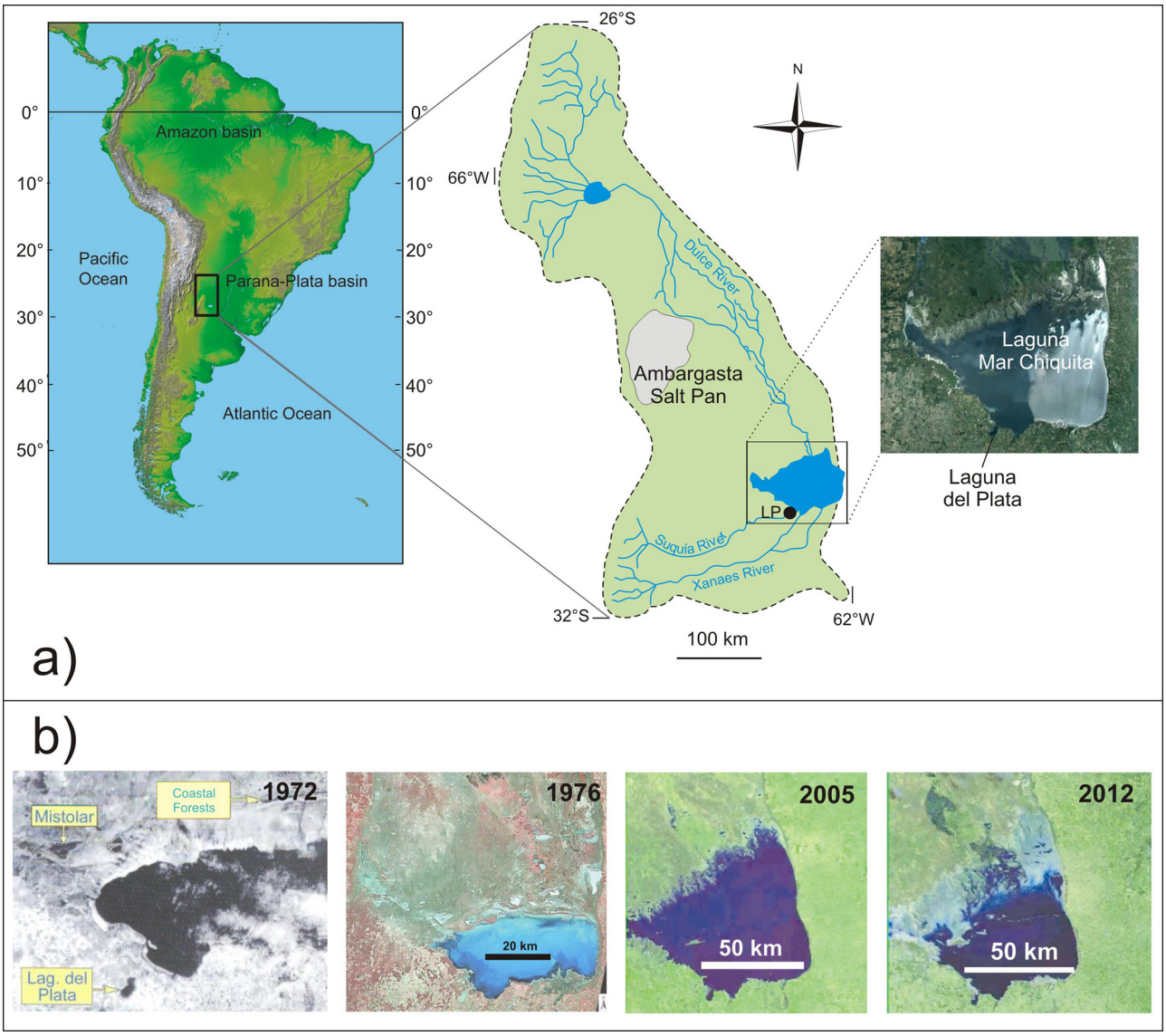

Fig. 1. (a) Study area with location of Laguna del Plata sediment core (LP) and (b) satellite images that show the size variation in the Laguna Mar Chiquita system.

(Gilli et al., 2005) and the effect of changes in insolation (Markgraf, 1998) that derived on the strengthening of the Southern Westerlies. The most intense magnitude was dated around 4.7 cal ka BP, this cold and dry phase of the Middle Holocene is consistent with a reduced latitudinal convey of moisture from the tropics to the subtropics as a consequence of a weakened Monsoonal circulation. These conditions extended until the middle of the first millennia when less extreme lowstands can be inferred by 1.5 cal ka BP (Kröhling and Iriondo, 1999). The timing of the droughts for both the first and second millennia is poorly resolved due to the occurrence of several sedimentary hiatuses indicated by gypsum-halite layers. In the middle part of the 18th Century (~A.D. 1770), sedimentation became more constant and a good chronology has been established for this latter part of the sequence based on ^{210}Pb dates (Piovano et al., 2002). This lowstand has been associated with the last part of the Little Ice Age whereas the lake level remained very low until the last quarter of the 20th century (i.e. decade of 1970s) when a hyperhumid period started.

The landscape in the region is characterized by Plio-Pleistocene alluvial fans progressing from the Sierras Pampeanas to the east (Kröhling and Iriondo, 1999). These sediments are covered by aeolian deposits of loessic sediments made of metamorphic and igneous rocks shards and volcaniclastic material derived from the Andes Cordillera, Sierras Pampeanas, Paraná basin and Uruguayan shield (Zárate, 2003) and transferred by southern winds that formed the Pampean Aeolian System (Brunetto and Iriondo, 2007). The uplift of the San Guillermo High, due to the activation of the Tostado-Selva fault in the Middle Pleistocene (Iriondo, 1989, 1997), and the accumulation of the fans of Suquía and Xanaes Rivers against it, closed the Dulce River thus generating the Mar Chiquita impounding (Costa, 1999; Mon and Gutierrez, 2009).

2.2. Sampling methods

The 120 cm sedimentary core LP (30°55′S, 62°51′W) was taken at Laguna del Plata (Fig. 1a), at 1.5 m water depth with an Eijkelkamp hand corer beeker (CICTERRA-UNC) which allows to maintain perfect conditions for transportation and maintain the core humid. At the EPOC laboratory (France), the core was stored in refrigerated dedicated room before to be opened, described, photographed, sliced longitudinally for radiographical study (Fig. 2a and b) and sampled each 0.5 cm. High-resolution 256 grey-level

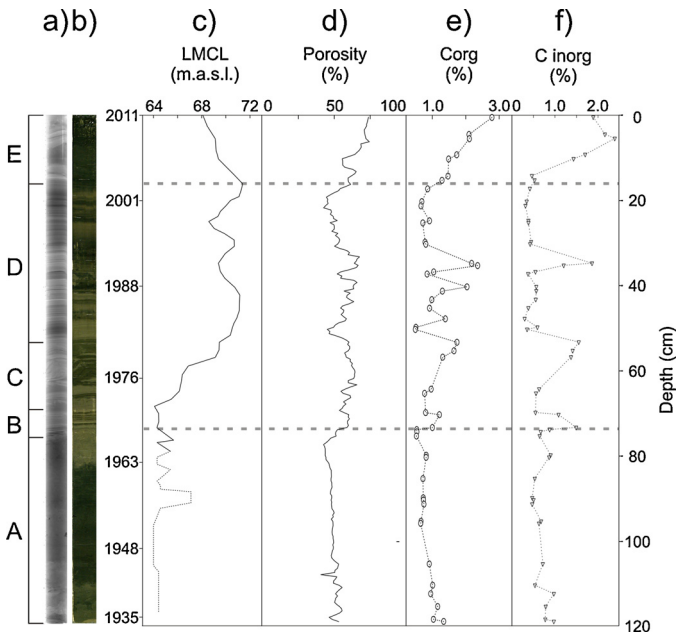

Fig. 2. Sedimentary units A to E where defined on the base of lamination indexes (LI). (a) Sediment core X-ray image, (b) sediment core photograph, (c) LMCL (Laguna Mar Chiquita level – the dashed line corresponds to reconstructed data developed in Piovano et al., 2002), (d) porosity record expressed in percentage, (e) organic carbon (C_{org}) content, and (f) inorganic carbon (C_{inorg}) content.

images were acquired with the automated X-ray core imaging system SCOPIX (Migeon et al., 1999 and Lofi and Weber, 2001). Porosity has been determined from the measure of the weight before and after drying at 50 °C for three days until constant weight, using an ultra precise balance (serie 32OXT, Precisa). Dry bulk density (DBD) was then calculated by using wet and dry weight, assuming the density of sediment grains to be 2.65 g cm^{-3}. Subsequently, samples were ground to 4-μm powder for further analysis.

2.3. Analytical methods

2.3.1. Total and organic carbon, major and minor elements

Total carbon and organic carbon (C_{org}) concentrations were determined with a LECO CS 125 analyzer by direct combustion in an induction furnace, and quantitative CO_2 detection by infrared absorption using ~50 mg dry sediment sub-samples without additional sample treatment (total carbon) or after carbonate elimination (organic carbon). For this, sample aliquots were acidified (2 N HCl) in ceramic crucibles, then dried at 60 °C for 24 h to remove inorganic carbon and most of the remaining acid and water previous to the combustion (Etcheber et al., 1999). Quality was checked by measuring certified reference materials (e.g. LECO 501–503) and intercalibrations (e.g. King et al., 1998).

Measures of Al, Si, K, Ti, Fe, Zr, Mn, Sr, S, Cl and Ca were performed by XRF using an Avaatech XRF core–scanner on one of the halves of the core at 1 mm resolution. The measurements were produced using 58 kV X-ray voltage and an X-ray current of 10 mA. The measurements obtained by XRF reflect the composition of a thin (sub-mm) layer on top of the sediment surface where the intensity of the different elements is expressed as counts per second (cps). The use of Al for this purpose allows monitoring and correcting the relative variations in the lithogenic component of the sediment (Löwemark et al., 2011; Liang et al., 2012) and additional sedimentary factors that influence XRF measurements (water content, surface roughness and grain size variations; Böning et al., 2007; Tjallingii et al., 2007; Weltje and Tjallingi, 2008). This technique does not allow quantification but relative variation of the elementary composition between different levels of the core or between cores. Its importance lies in the fact that is a non-destructive technique and allows to obtain a bulk-sediment chemistry data and main geological variations (Tjallingii et al., 2007; Montero-Serrano et al., 2010).

2.3.2. Radionuclides

Activities of ^{210}Pb, ^{232}Th, ^{226}Ra and ^{137}Cs were measured using a low background, high efficiency, well-shaped γ detector (CANBERRA) (Schmidt et al., 2009). Calibration of the γ detector was achieved using certified reference materials (IAEA-RGU-1; IAEA-RGTh; SOIL-6). Activities are expressed in mBq g^{-1} and errors are based on 1 SD counting statistics. Excess ^{210}Pb ($^{210}Pb_{xs}$) was calculated by subtracting the activity supported by its parent isotope, ^{226}Ra, from the total ^{210}Pb activity in the sediment.

2.3.3. Total particulate Hg

Total Particulate Hg (Hg_{TP}) concentration was determined on ~70–100 mg aliquots of dry sediment by cold vapour atomic absorption spectrometry after incineration (O_2 stream) and amalgamation, using a Direct Mercury Analyzer (MILESTONE, DMA 80). The quality of the analytical results was systematically checked analyzing international certified sediment reference materials (LKSD-4, IAEA 433, 1646a) every set of 5 samples and concentrations were expressed in μg kg^{-1} dry weight. The detection limit (3 times the standard deviation of 5 blank values) varied daily from 1 to 2 μg kg^{-1}.

2.3.4. Selective extractions

Selective extractions are commonly used in order to determine trace element distribution in different solid phases (soils and sediments) by extracting different operationally-defined fractions following either sequential (Tessier et al., 1979; Sahuquillo et al., 2003) or parallel extraction schemes (Audry et al., 2005). In this study, Hg distribution on different solid carrier phases was operationally assessed by 3 parallel or single chemical extractions, i.e. using each reagent on a different sample aliquot (Farrah and Pickering, 1993; Alborés et al., 2000), as described in Castelle et al. (2007). Parallel extraction schemes avoid certain limitations such as (i) metal transfer from one phase to the another (Bermond, 1992), (ii) multiple risks of sample contamination from successive reagents used (Quevauviller, 1998), (iii) possible changes in elemental speciation during the successive extraction steps and (iv) changes or losses of elemental species during the residue washing step (Rosenberg and Ariese, 2001). Besides, this method shows no risk for sample losses and an error occurred during one extraction does not compromise the entire schema (Tack et al., 1996). A brief summary with the details of the three different operationally-defined fractions is listed in Table 1.

For all the analyses indicated above, solutions prepared with analytical reagent grade chemicals and purified water (Milli-Q® system) were used. Labware in contact with the samples were acid cleaned (soaked in 10% HCl during 3 days, rinsed 3 times with Milli-Q® water and dried under a laminar flow hood) before proceeding with laboratory work.

2.3.4.1. Ascorbate extraction (reducible fraction). This reducing single extraction removes trace elements associated with Mn oxides and the most reactive Fe oxide fraction (i.e. amorphous oxides; Kostka and Luther, 1994; Audry et al., 2006), using a 0.11 M ascorbate reagent (5:5:2 sodium citrate/sodium-bicarbonate/ascorbic-acid mixture; J.T. Baker, Baker analyzed/J.T. Baker, Baker analyzed/Acrôs Organics).

2.3.4.2. H_2O_2 extraction (oxidizable fraction). The oxidizing single extraction using hydrogen peroxide (H_2O_2) typically extracts organic matter but sulphides are also partially oxidized during this

Table 1
Operating conditions applied for the single extraction procedures.

Fraction	Sample weight (mg)	Reagent	Shaking time, temperature
Ascorbate extraction – reducible fraction	200	12.5 ml of ascorbate solution	24 h, 25 °C
H_2O_2 extraction – oxidizable fraction	250	8 ml of 30% H_2O_2 + NaOH (pH 5) Then 3 ml of 30% H_2O_2 + NaOH Then 5 ml of 5 M NH_4OAc + 20 ml H_20 Milli-Q	5 h, 85 °C 3 h, 85 °C 30 min, 25 °C
HCl extraction – acid-soluble/reactive fraction	200	12.5 ml of 1 N HCl	24 h, 25 °C

step (Tessier et al., 1979). This work utilizes a modified Tessier protocol (Ma and Uren, 1995; Audry et al., 2006), previously applied for Hg solid speciation (Castelle et al., 2007).

2.3.4.3. HCl extraction (acid-soluble/reactive fraction). The so-called reactive (1 M HCl acid-soluble) fraction comprises metals associated with amorphous and crystalline Mn and Fe oxides, carbonates, hydrous Al silicates and acid volatile sulphides (AVS) (Huerta-Díaz and Morse, 1990, 1992; Nova-López and Huerta-Díaz, 2001) not including the oxidation products of Fe monosulphides (goethite and hematite; Raiswell et al., 1994). Acid volatile sulphide (AVS) is operationally defined as the fraction of sulphides that is extractable by 1 or 6 M cold HCl. The acid-soluble fraction was also empirically designated to extract most of the potentially bioavailable trace metals (Bryan and Langston, 1992; Langston et al., 1999).

In the final step of each individual extraction procedure, the tubes were centrifugated for 15 min at 3000 rpm, and the residual sediment was rinsed twice with Milli-Q® water, dried at 50 °C and homogenized in an agate mortar. The residual Hg fraction was measured with the DMA (as described above) and subtracted from the Hg_{TP} to evaluate each extracted Hg fraction.

3. Results

3.1. Textural, physical and chemical properties of Laguna del Plata core

Laguna del Plata (LP) sedimentary core is characterized by the alternance of dark and light grey lamination (Fig. 2a). The core description is based on four values of lamination indexes (LI) proposed by Piovano et al. (2002). Continuous laminae up to 2 mm thick are designated by "1", diffuse or discontinuous 2–4 mm thick by "2", thin banded 4–10 mm thick by "3" and finally thick banded >10 mm thick by "4". When there is an absence of lamination the sedimentation is called massive. Fig. 2 shows a photograph and X-ray radiograph image of the LP core that summarizes its main sedimentological features. Thus, 5 sedimentary units could be recognized. The first one (A) is a massive sequence that extends from the bottom up to 75 cm with a net contact. From the base of the core to the top this sequence shows different colours on the photograph: light green colour in deepest part, followed by a dark green olive colour that overlies and a very light green colour on the top of it. In the X-Ray image the colour varies from light grey in the bottom to darker grey in the upper part. A small sequence characterized by LI2 (B) from 75 to 69 cm shows lamination due to an alternance of dark to light colours sediments. Overlying this sequence up to 53 cm there is an alternance of LI4 (C) with a predominance of a light colour. From here up to 16 cm a sequence of LI1 and LI2 laminations (D) are intercalated with a small LI3 lamination located at 27–39 cm. There is an alternance of dark to light grey making more visible the contacts between laminations. The upper part of the core shows a LI4 sequence (E) with a dark olive green colour in the picture (Fig. 2).

Some physical and chemical characteristics of the core are shown in the profiles of Fig. 2. The level with the lowest porosity value (40.0%) occurred near the bottom of the LP core, while the highest (75.5%) was registered near the top. Thus three zones could be described (light grey dashed lines in Fig. 2): from the bottom to 74 cm the porosity present average values of 48.4 ± 2.9%, from 74 to 16 cm porosity raised up to 56.2 ± 6.1% remaining nearly constant and finally the first 16 cm are represented by an abrupt augmentation of water percentage (from 59.9 to 74.5%). Lamination seems to be related to this change in porosity: section A to the lower porosity, B, C and D to the intermediate porosity and E with the highest one.

Organic carbon (C_{org}) values ranged between ~0.5 and ~2.8%. This parameter seems to follow the same tendency of porosity. From 120 to 74 cm C_{org} values remained practically constant around ~0.8% ± 0.2, up to 30 cm values suffered a big fluctuation between 0.5 and 2.4%, being synchronous with porosity variations. The last centimetres are given by the highest values with its maximum of 2.8% in the top of the core. Inorganic carbon (C_{inorg}) profile shows a similar behaviour to C_{org}. Its contents (Fig. 2f) vary from 0.3 to 2.4% along the core. From 120 to 74 cm the average value is 0.7 ± 0.2%, from 74 to 16 cm it is 0.7 ± 0.5% and in the last 16 cm the average value is 1.5 ± 0.8%.

XRF elemental profiles depict mainly three domains (Fig. 3). The lower part of the core from the base up to 74 cm is characterized by a signal that remains almost constant except for Zr, S, Ca and Sr that rises in the last centimetres. The second domain shows a high fluctuation visible in all the measured elements that extends in the central part of the core up to 16 cm. From here up to the top Al, Si, K, Ti, Mn, Fe and Zr show a diminution in the signal while for Sr, S, Cl and Ca the opposite occurs.

3.2. Radionuclides

The ^{210}Pb ($T_{1/2}$ = 22.3 years) is a naturally occurring radionuclide delivered continuously to the landscape by atmospheric fallout (Saari et al., 2010) and becomes rapidly and strongly bound to particulate matter. This atmospherically derived ^{210}Pb scavenged by particles (Fig. 4), is referred to ^{210}Pb in excess ($^{210}Pb_{xs}$) of that supported within particles by the decay of its parent isotope, ^{226}Ra. In LP core these excess activities range from 5 to 72 mBq g^{-1}. There is a general trend in decreasing $^{210}Pb_{xs}$ as expected due to the decay of the unsupported ^{210}Pb. This decrease presents some irregularities, as observed at about 24 cm where excess is lower when compared to the surrounding layers. The long-lived and naturally occurring ^{232}Th is usually associated with the detrital fraction (van der Klooster et al., 2011), therefore activity changes can be an indication of different lithological sources or proportions. ^{232}Th activities range between 26 and 42 mBq g^{-1}, the lowest values are usually observed in the upper 20 cm. This section presents also the highest total carbon content that is likely to dilute the detrital fraction. It is also noticeable that low $^{210}Pb_{xs}$ at 24 cm is associated with a high ^{232}Th activity. Such a high ^{232}Th are mostly observed in the deepest part of the core, at >70 cm depth.

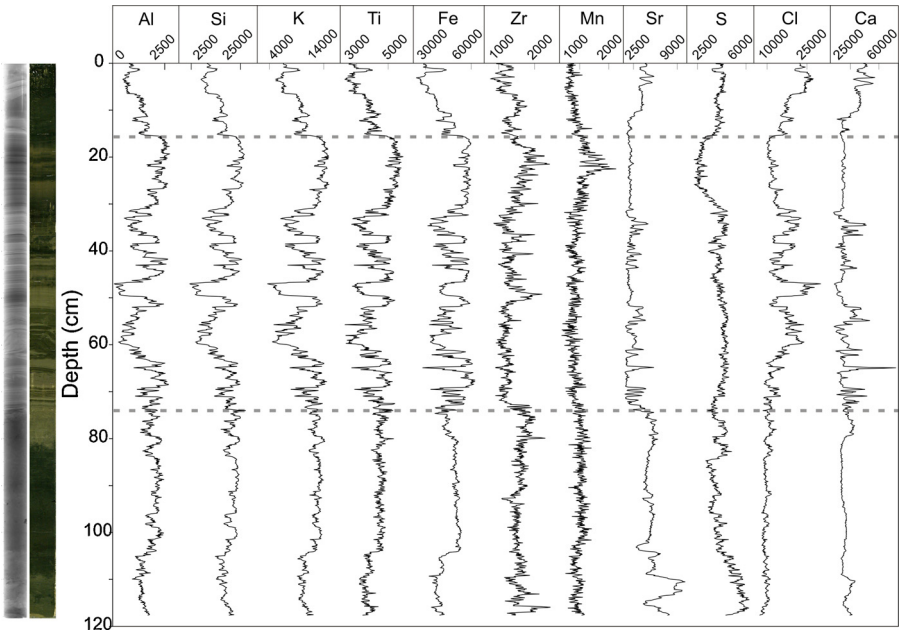

Fig. 3. XRF logs from Laguna del Plata. The values are given in counts per second (cps).

On the opposite, ^{137}Cs ($T_{1/2}$ = 30 years) is an artificial radionuclide: its occurrence in the environment is primarily the result of the nuclear weapon test fall-out in the early sixties, and in Europe of the Chernobyl accident in 1986 of well-known pulse inputs (UNSCEAR, 2000). At present, atmospheric fluxes are almost negligible (Quintana, 2011). Sedimentary profile of ^{137}Cs in core presents the expected shape with a peak in depth and negligible activities in the uppermost section (<1 mBq g^{-1}). The maximum activities are recorded around 75–80 cm, with values up to 26 mBq g^{-1}. Below that peak, ^{137}Cs disappears rapidly to negligible levels below 85 cm.

3.3. Hg concentrations

Total particulate Hg (Hg_{TP}) concentrations measured every 0.5 cm interval along the Laguna del Plata core, varied between ~13 and ~131 μg/kg (Fig. 5a). In the deepest part of the core (from 120 to 74 cm) the lowest and most constant concentrations occurred (an average of 17.242 ± 1.730 μg kg^{-1}). From this point to the surface Hg_{TP} values are variable. From 74 cm up to 45 cm they show average concentrations of 42.381 ± 14.602 μg kg^{-1}, beyond this level distinct peaks of 89.701, 131.470 and 87.260 μg kg^{-1} are shown at 43.2, 36.7 and 30.2 cm respectively. In most recent sediments (~16–0 cm), the average concentration is 65.611 ± 16.017 μg kg^{-1}.

Hg concentration associated to the reductible fraction was negligible throughout the core, while the Hg in both acid-extracted (1 M HCl) and oxidizable fractions accounted for the major part of the Hg_{TP} values measured in the sediments.

The relation between Hg_{HCl} and Hg_{TP} showed two different patterns (Fig. 5b): (i) from the bottom of the core to 74 cm, Hg_{HCl} accounted in average for 42.844 ± 22.334% of Hg_{TP} and (ii) above 74 cm to the top, Hg_{HCl} represented in average 21.437 ± 13.702% of Hg_{TP}. Similar to Hg_{HCl}, the relative contribution of Hg_{H2O2} to Hg_{TP} changed with depth (Fig. 5c) showing in average the highest values of 76.687 ± 11.021% in the lower part of the core up to 40 cm. Above, the relative contribution of Hg_{H2O2} to Hg_{TP} was clearly lower but still represented 56.623 ± 15.052%.

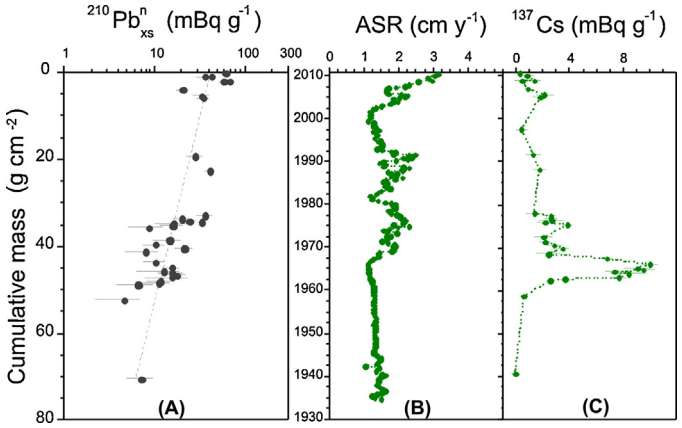

Fig. 4. (a) Normalized ^{210}Pbxs against cumulative mass: the dashed line corresponds to the exponential regression used to determine mass accumulation rate (MAR), (b) average sedimentation rate (ASR) and (c) ^{137}Cs plotted against calendar ages, based on ^{210}Pb dating.

4. Discussion

4.1. Sediment deposition and chronology

Use of ^{210}Pb has been widely done to calculate short-term (years to decades) sediment accumulation rates in continental and oceanic environment since the last 40 years (Appleby, 2001). Dating is calculated using excess activity of ^{210}Pb ($^{210}Pb_{xs}$) which is incorporated rapidly into the sediment from atmospheric fallout and water column scavenging. Once incorporated into the sediment, unsupported ^{210}Pb decays with time in the sediment column according to its half-live, by Eq. (1):

$$^{210}Pb_{xs(z)} = {}^{210}Pb_{xs(0)}e^{-\lambda t} \quad (1)$$

where $^{210}Pb_{xs(z)}$ and $^{210}Pb_{xs(0)}$ represent the excess ^{210}Pb at the sediment–water interface, or at the base of the mixed layer, and at the depth z, λ is the ^{210}Pb decay constant (0.0311 y^{-1}), and t is the age in years. Several models have been developed to calculate an age or accumulation rate (Sanchez-Cabeza and Ruiz-Fernández, 2012, among others): CIC (constant initial concentration); CSR (constant rate of supply); CFCS (constant flux-constant sedimentation). The Constant Initial Concentration (CIC) model in which the

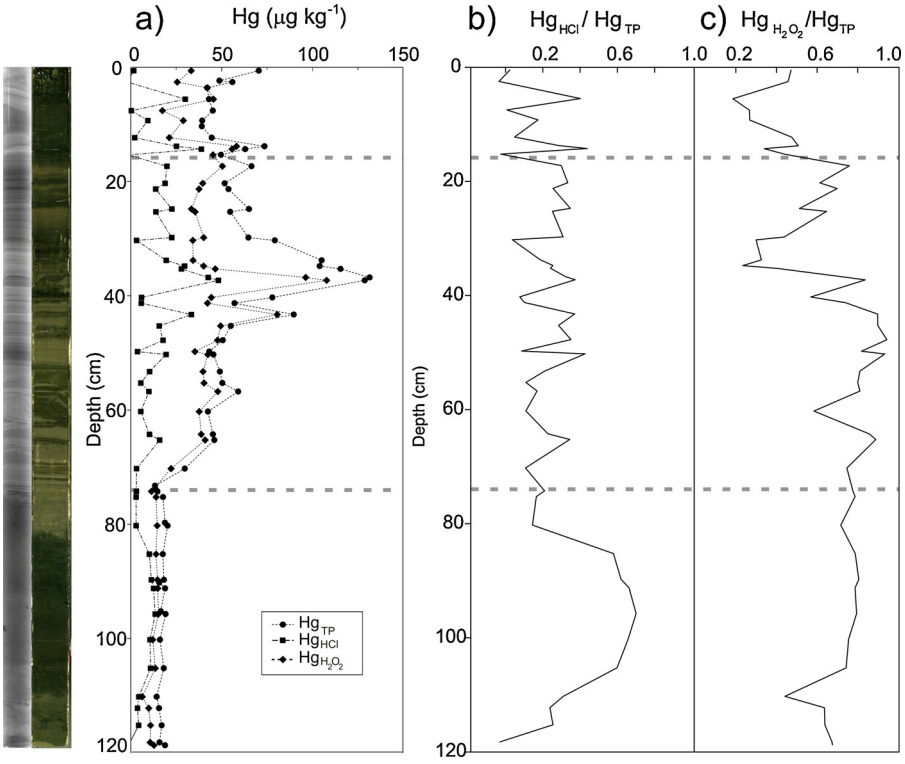

Fig. 5. Mercury concentrations. (a) Selective extractions corresponding to the total particulate (Hg_{TP}), oxidiable (Hg_{H2O2}) and acid-soluble/reactive (Hg_{HCl}) fractions.

sediments have a constant ^{210}Pb concentration regardless the accumulation rates (Appleby, 2001) was left behind due to that Laguna del Plata has suffered alternated connections and disconnections from Laguna Mar Chiquita influencing the amount and nature of the sedimented material (Piovano et al., 2002). Thus the CFCS model was chosen to calculate the sedimentation rates and age for the lake under the two basic assumptions: ^{210}Pb atmospheric deposition and the mass accumulation are constant. The mass accumulation rate (MAR, g cm^{-2} y^{-1}) can be obtained considering Eq. (2)

$$^{210}Pb_{xs(z)} = {}^{210}Pb_{xs(0)}e^{-m}(z)\frac{\lambda}{MAR} \quad (2)$$

where $m(z)$ is the cumulative dry mass per unit area (g cm^{-2}) at depth z. To compensate the effect of composition changes of sediment, $^{210}Pb_{xs}$ activities were normalized by using ^{232}Th concentrations, measured at the same time through gamma, thus limiting the errors. MAR was calculated from the slope of the exponential regression of $^{210}Pb^{n}_{xs}$ plotted against cumulative mass (Fig. 4a). The average mass accumulation rate is 1.0 g cm^{-2} y^{-1}. The sedimentation rate (in years) has been calculated by dividing the cumulated dry mass per unit area by the mass accumulation rate, allowing to estimate the average sedimentation rates (ASR) (Fig. 4b). The expected deposition year for each sediments layer was calculated considering the sampling year (2011) and the water-sediment interface at the uppermost layer as a reference for establishing the chronology.

Robbins and Eddington (1975) showed that it is necessary to confirm the accuracy of the ^{210}Pb-based model using an independent time-stratigraphic marker, such as fallout ^{137}Cs. The ^{137}Cs profile was plotted as a function of the time scale based on ^{210}Pb (Fig. 4c). It is noticeable that the peak of ^{137}Cs in core LP corresponds to the year 1966, which is in close agreement with the annual atmospheric fallout of ^{137}Cs recorded at Buenos Aires around 1960 (Quintana, 2011). In general the sedimentary ^{137}Cs record mimics rather well the atmospheric fallout, validating the chronology derived from ^{210}Pb and coinciding with the abrupt hydrological changes that the lake system have been through during the decade of 1970s.

Sedimentation rates are comprised between 1 and 3 cm y^{-1}, being rather variable with depth. They are less than 2 cm y^{-1} in the deepest part and the highest are located in the uppermost part of the core. What occurs in the lower part of the core is mainly ascribed to sediment compaction and associated with a simultaneous decrease in porosity. During the period covering the early 1970s to the early 1990s, ASR shows strong variability, which may be in relation to environmental changes and the continuous connection of Laguna del Plata to Laguna Mar Chiquita that happened after 1975 during the onset of the last highstand (see Fig. 1b Satellite images). In the lowermost layers of the core, sedimentation rates display rather constant values, around 1.2–1.5 cm y^{-1}, and are likely to indicate constant sedimentation conditions during lowstand lake scenarios with low fluvial input.

Chemical data given by XRF helps to understand the changes that Laguna del Plata sediments composition experienced during the last six decades. In concordance with previous observations performed by Piovano et al. (2004b) in cores retrieved from Laguna de Mar Chiquita and Laguna del Plata, the elemental variations described in Fig. 3 seem to be controlled by well-known hydrological fluctuations. For comparison purposes, Laguna Mar Chiquita level record was considered because there is no a continuous record for Laguna del Plata lake and both are controlled by the same hydrological balance (Troin et al., 2010). The bottom part of the core up to 74 cm corresponds to the sedimentary record before ~1970 where LP was completely isolated from LMC and the inputs were mainly from the Suquía River. The almost constant XRF signals at the lowermost part of the core reflect this single contribution to the sedimentary record (Fig. 3). The onset of higher regional precipitations since ~1970, generated the connection of both lakes by 1976 that persist nowadays (Fig. 1b), changing the sedimentation pattern overall the Laguna Mar Chiquita system (Piovano et al., 2002,

2004a). Rising lake level likely triggered the strong variations in Si, K, Ti, Fe, and Zr concentrations measured in the core between 74 and 16 cm depth, reflecting a high contribution of detrital input due to soil or fluvial-bank erosion suffered in the catchment. Several authors (Rothwell and Rack, 2006; Böning et al., 2007; Moreno et al., 2007; Löwemark et al., 2011) coincide that variations of terrigenous elements such as Al, Si, K, Fe, and Ti are likely the consequence of inputs of allocthonous materials. In addition, an increase in the lake primary productivity during highstands, marked by changes in the C_{org} % (Fig. 2e), may additionally control the porosity values.

4.2. Historical record of Hg and its solid carrier phases in sediments of Laguna del Plata

Hg levels measured in the Laguna del Plata sediments (Fig. 4) were much lower than those typically reported for contaminated freshwater or marine areas (e.g. Streets et al., 2005; Castelle et al., 2007; Larrose et al., 2010; Elbaz-Poulichet et al., 2011). Given the fine-grained nature of the sediment, such Hg_{TP} levels are clearly within the range of those attributed to weakly contaminated systems (e.g. Schäfer et al., 2006).

Like for the other parameters discussed above, the variations of Hg and its main solid carrier phases observed in the Laguna del Plata core are due to both changes in lake hydrology and general atmospheric deposition, rather than pollution point sources in the watershed.

The sediments accumulated in the lake before the 1970s show rather constant and very low Hg_{TP} concentrations. During this period of high aridity and low lake levels, particles transported by the Suquía River exclusively settled in the Laguna del Plata due to the absence of hydraulic links between the latter and Laguna Mar Chiquita. The high Hg_{HCl} fraction (>40% of Hg_{TP}) combined with the relatively high Hg_{H202} fraction (76.4 ± 11.6%) shows that most of Hg_{TP} measured in the sediments is associated with secondary sulphides, especially in the 105–85 cm depth range (Fig. 5c). This is consistent with X-ray diffractometry data that shows the presence of pyrite at the base of the core (data not shown) which indicates that precipitation of authigenic sulphides occurred under dominant anoxic conditions produced by bacterial activity at the water-sediment interface. Elevated salinity (380 g L^{-1}; Piovano et al., 2004a) and alkaline chloride–sulphate sodium type waters (Martínez, 1991) represent the geochemical conditions predominating during lake lowstands. Hg associated with the residual fraction not extracted by the single extraction approach, i.e. attributed to the non-reactive crystalline matrix, was very low (close to zero) in the sediments before the 1970s, indicating that nearly all Hg deposited during that period was potentially bioavailable.

In the uppermost part of the core (74–0 cm), i.e. in sediments accumulated from the 1970s, Hg_{TP} concentrations were clearly higher than downcore. This situation coincides with the beginning of an increasingly humid period in the region, and concomitant rise in the lake system levels. Increased erosion and riverborne particle transport in the Suquía River watershed also occurred during this period.

In the 74–40 cm depth range, maximum Hg_{H202} and clearly lower Hg_{HCl} indicate that Hg is mainly associated with sedimentary organic matter, which is consistent with increasing lake primary productivity (Da Silva et al., 2008) but also with increasing erosion and particle transport in the Suquía River (Piovano et al., 2009). The highly variable Hg_{HCl} relative to Hg_{TP} in the top 74 cm of the core reflects episodes of intense erosion with changing proportions of Hg associated with clay minerals and Mn and Fe oxy-hydroxides transported from the catchments. Hydrochemical conditions in the lake during highstands corresponded to alkaline chloride–sulphate sodium type waters, supersaturated in calcite and occasionally in gypsum (Martínez et al., 1994).

Hg profile shows maximum Hg_{TP} at ~38 cm, i.e. in the depth range roughly attributed to records of the years 1990–1995. The residual Hg fraction shows maximum levels (>50% of Hg_{TP}) at ~35 cm depth, suggesting an episode with major transport and deposition of non-reactive Hg-bearing phases during the 1990s just after the episode responsible of the Hg_{TP} maximum. Accordingly, the maximum Hg_{TP} levels together with minimum Hg_{H202}/Hg_{TP} and relatively low Hg_{HCl}/Hg_{TP} indicate dominance of Hg-bearing phases not determined by the used selective extractions. Among the different Hg sources described in natural systems, volcanic emissions are a major issue (i.e. Fitzgerald and Lamborg, 2003; Selin, 2009). Due to the proximity to the Andean volcanic system and its well known influence on the study area (e.g. Gaiero et al., 2007; Osores et al., 2011) volcanic eruptions could account for this observation. In fact, the eruption record of the past 100 years indicates that the observed peak may reflect Hg inputs from the eruption of the Hudson and Láscar volcanoes occurred in 1991 and 1993 respectively. The Hudson volcano is located in Chile at 45°54′S to 72°58′W. This volcano erupted in two phases in August 1991, producing 4.3 km^3 of pyroclastic material during one of the major eruptions of the 20th century (Wilson et al., 2011). The ashes from the first eruption moved mainly in NNE to NE direction (Kratzmann et al., 2008, 2010) and reaching the Laguna del Plata. Unfortunately it is not possible to define the limits of the plume with certitude due to its low ash content (Constantine et al., 2000). Láscar volcano is located at 23°22′S to 67°44′W and started its activity in 1984 culminating with a major explosive eruption in April 1993. This last eruption generated a column between 5 and 25 km above the volcano and tephra ashes reached Buenos Aires located 1500 km to the southeast (Matthews et al., 1997). With these plumes arriving to the study area, the Hg associated to volcano-clastic particles settled as wet or dry deposition in the Suquía River watershed. This is in agreement with the peak of Hg_{TP} observed in the core (between 37.2 and 30.2 cm) and its preferential association with non-reactive particles in the sediments accumulated in the years following the eruption.

The hydrological model of the Laguna del Plata system proposed by Piovano et al. (2004a,b) for the last century, was modified in order to show the inputs of the main Hg-bearing phases identified in the area (Fig. 6). Precipitation (P) and evaporation (E) are represented with arrows, whose relative lengths are proportional to their volume. The higher river runoff that occurred after the 1970s is indicated by a solid arrow, whereas dotted arrow indicate comparatively low inputs that prevailed in the dry period. The thickness of the arrows associated with different Hg-bearing phases recognized in the studied area, is proportional to their respective importance. During the dry conditions that predominated in the study area before the 1970s, inputs of Hg to the lake corresponded mainly to contributions from natural sources such as atmospheric Hg (dry deposition) and Hg-bearing particles (particularly sulphides) that were transported to the lake from the Suquía River upper basin. Under high stand conditions (after 1970s), these two sources increased their contributions due to increasing precipitation (wet deposition) and higher soil erosion in the catchments, but also to increasing global Hg flux. The more humid conditions lead to increased lake primary productivity and hence, a higher affinity of Hg for organic matter particle is found in sediments accumulated during this period.

The sources of Hg in the Laguna del Plata sediments are mostly assigned to natural sources, but also a minor contribution from global Hg inputs should be considered, as well as from some other local anthropogenic sources, that became increasingly important after the 1970s when an incipient industrial development started in the region.

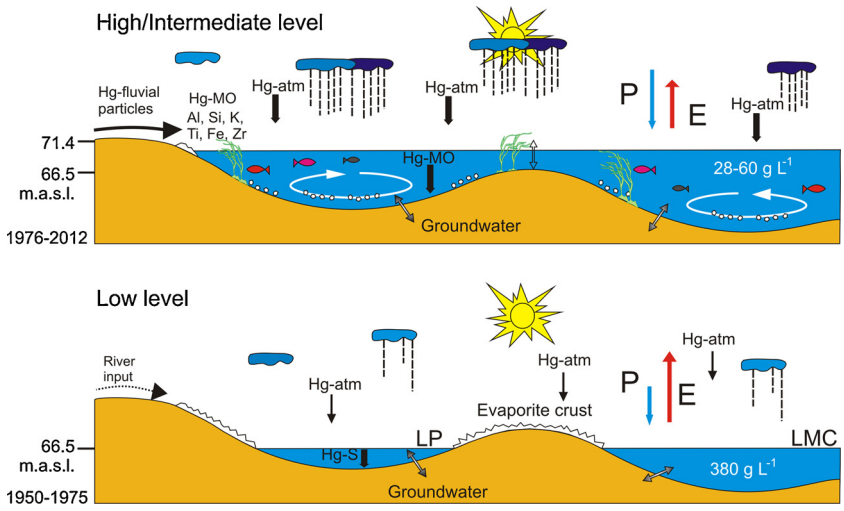

Fig. 6. Schematic section of Laguna del Plata (LP) and Mar Chiquita (LMC) system showing Hg and other elements cycles under different hydrological stages. Modified from Piovano et al. (2004). Length and thickness of the arrows are proportional to the components contribution. Hg-atm: atmospheric Hg; Hg-S: Hg-bearing sulphides, Hg-OM: Hg-bearing organic matter.

5. Conclusions

Sedimentary record in Laguna del Plata shows a highly variable sedimentation regime in the last ~80 years, controlled by changes in the regional hydrological balance. These changes also triggered variations in the chemical composition of the sediments. Among the analyzed elements, Hg was used as a potential marker of the natural and atrophic activities.

Before the 1970s, LP was completely isolated from LMC and the inputs of sediments were mainly from the Suquía River. During this period, the occurrence of highly saline waters and anoxic conditions at the water-sediment interface, promoted the precipitation of Hg-bearing sulphides. In the following years, the more humid conditions enhanced primary productivity in the lake, driving increased organic matter contents in the sediment record. Hg accumulated during this period, was preferentially associated with the organic fraction of the sediments. The upper centimetres of the core show increasing Hg concentrations that are considered to be closely related to the industrial development of the region but also to the increasing influence of global Hg fluxes.

The highest Hg_{TP} values are found at ~35 cm depth (corresponding to the years 1990–1995) where the Hg_{H2O2}/Hg_{TP} and Hg_{HCl}/Hg_{TP} relations are also relatively low. This suggests a contribution from a Hg-bearing source that is not affected by the applied extraction methods. More than a punctual source of pollution, this peak is likely related to two eruptive events occurred in the Andean Cordillera in this period: the eruption of Hudson volcano in southern Patagonia that occurred in 1991 and the one of the Láscar volcano in northern Chile that occurred in 1993. In both cases, the respective ash plumes were documented to have reached the Laguna del Plata region.

Acknowledgments

This work is in the frame of a doctoral thesis financed by ERASMUS MUNDUS External Cooperation Window, lot 18-BAPE-Bolivia, Argentina, Peru and Europe. Field trips were financed with funds from PIP 112-200801-00808 (CONICET-Argentina). The authors want to thank equally to the reviewers and their constructive remarks.

References

Aceituno, P., 1988. On the functioning of the Southern Oscillation in the South American sector. Part I: surface climate. Monthly Weather Review 116, 505–524.
Alborés, A.F., Cid, B.P., Gómez, E.F., López, E.F., 2000. Comparison between sequential extraction procedures and single extractions for metal partitioning in sewage sludge samples. Analyst 125, 1353–1357.
Amin, O., Ferrer, L., Marcovecchio, J., 1996. Heavy metal concentrations in litteral sediments from the Beagle Channel, Tierra del Fuego, Argentina. Environmental Monitoring and Assessment 41 (3), 219–231.
Appleby, P.G., 2001. Chronostratigraphic techniques in recent sediments. In: Last, W.M., Smol, J.P. (Eds.), Tracking Environmental Change Using Lake Sediments, Basin Analysis, Coring, and Chronological Techniques, vol. 1. Kluwer Academic Publishers, Dordrecht, The Netherlands.
Arribére, M.A., Ribeiro Guevara, S., Sánchez, R.S., Gil, M.I., Román Ross, G., Daurade, L.E., Fajon, V., Horvat, M., Alcalde, R., Kestelman, A.J., 2003. Heavy metals in the vicinity of a chlor-alkali factory in the upper Negro River ecosystem, Northern Patagonia, Argentina. Science of the Total Environment 301 (1–3), 187–203.
Audry, S., Blanc, G., Schäfer, J., 2005. The impact of sulphide oxidation on dissolved metal (Cd, Zn, Cu, Cr, Co, Ni, U) inputs into the Lot-Garonne fluvial system (France). Applied Geochemistry 20 (5), 919–931.
Audry, S., Blanc, G., Schäfer, J., 2006. Solid state partitioning of trace metals in suspended particulate matter from a river system affected by smelting waste drainage. Science of the Total Environment 363, 216–236.
Balcom, P., Fitzgerald, W., Hammerschmidt, C., Lamborg, C., Graham, L., 2004. Mercury sources and speciation in the waters of New York/New Jersey Harbor Estuary. Mater. Geoenviron. 51, 795–798. Environmental Technology 13 (12), 1175–1179.
Bermond, A.P., 1992. Thermodynamics applied to the study of the limits of sequential extraction procedures used for the speciation of trace elements in sediments and soils. Environmental Technology 13 (12), 1175–1179.
Biester, H., Bindler, R., Martinez-Cortizas, A., Engstrom, D.R., 2007. Modeling the past atmospheric deposition of mercury using natural archives. Environmental Science and Technology 41, 4851–4860.
Böning, P., Bard, E., Rose, J., 2007. Toward direct, micron-scale XRF elemental maps and quantitative profiles of wet marine sediments. Geochemistry, Geophysics, Geosystems 8 (5), http://dx.doi.org/10.1029/2006GC001480.
Botté, S.E., Freije, R.H., Marcovecchio, J.E., 2010. Distribution of several heavy metals in tidal flats sediments within Bahía Blanca Estuary (Argentina). Water, Air and Soil Pollution 210, 371–388, http://dx.doi.org/10.1007/s11270-009-0260-0.
Boulanger, J.-P., Leloup, J., Penalba, O., Rusticucci, M., Lafon, F., Vargas, W., 2005. Observed precipitation in the Paraná-Plata hydrological basin: long-term trends, extreme conditions and ENSO teleconnections. Climate Dynamics 24, 393–413.
Brunetto, E., Iriondo, M.H., 2007. Neotectónica en la Pampa Norte (Argentina). Revista de la Sociedad Geológica de España 20 (1–2), 17–29.
Bryan, G.W., Langston, W.J., 1992. Bioavailability, accumulation and effects of heavy metals in sediments with special reference to United Kingdom estuaries: a review. Environmental Pollution 76 (2), 89–131.
Bucher, E.H., Gavier Pizarro, G., Curto, E.D., 2006. In: Bucher, E.H. (Ed.), Cap. 1. Síntesis geográfica. En: Bañados del Río Dulce y Mar Chiquita (Córdoba, Argentina). Academia Nacional de Ciencias, Córdoba, Argentina, pp. 15–27.
Castelle, S., Schäfer, J., Blanc, G., Audry, S., Etcheber, H., Lissalde, J.-P., 2007. 50-year record and solid state speciation of mercury in natural and contaminated reservoir sediment. Applied Geochemistry 22, 1359–1370.

Constantine, E.K., Bluth, G.J.S., Rose, W.I., 2000. TOMS and AVHRR observations of drifting volcanic clouds from the August 1991 eruptions of Cerro Hudson. In: Mouginis-Mark, P., Crisp, J.A., Fink, J.H. (Eds.), Remote Sensing of Active Volcanism. Geophysical Monograph, Washington, DC, pp. 45–64.
Costa, C., 1999. Tectónica cuaternaria en las Sierras Pampeanas. Geología Argentina. Anales 29. Subsecretaría de Minería de la Nación. Servicio Geológico Minero Argentino. Instituto de Geología y Recursos Minerales, Buenos Aires.
Da Silva, L.S.V., Piovano, E.L., Azevedo, D. d.A., Aquino Neto, F.R. d., 2008. Quantitative evaluation of sedimentary organic matter from Laguna Mar Chiquita, Argentina. Organic Geochemistry 39 (4), 450–464.
De Marco, S.G., Botté, S.E., Marcovecchio, J.E., 2006. Mercury distribution in abiotic and biological compartments within several estuarine systems from Argentina: 1980–2005 period. Chemosphere 65, 213–223.
Depetris, P.J., Kempe, S., Latif, M., Mook, W.G., 1996. ENSO controlled flooding in the Paraná River (1904–1991). Naturwissenschaften 83, 127–129.
Diaz, E., 2000. Mercury pollution at gold mining sites in the Amazon environment. In: Principles of Environmental Toxicology. University of Idaho, 24 pp.
Downs, S.G., Macleod, C.L., Lester, J.N., 1998. Mercury in precipitation and its relation to bioaccumulation in fish: a literature review. Water, Air and Soil Pollution 108, 149–187.
Etcheber, H., Relexans, J.-C., Beliard, M., Weber, O., Buscail, R., Heussner, S., 1999. Distribution and quality of sedimentary organic matter on the Aquitanian margin (Bay of Biscay). Deep-Sea Research II 46, 2249–2288.
Elbaz-Poulichet, F., Dezileau, L., Freydier, R., Cossa, D., Sabatier, P., 2011. A 3500-year record of Hg and Pb contamination in a mediterranean sedimentary archive (The Pierre Blanche Lagoon, France). Environmental Science and Technology 45 (20), 8642–8647.
Farrah, H., Pickering, W.F., 1993. Factors influencing the potential mobility and bioavailability of metals in dried lake sediments. Chemical Speciation and Bioavailability 5 (3), 81–96.
Fitzgerald, W.F., Mason, R.P., 1997. Biogeochemical cycling of mercury in the marine environment. In: Sigel, H., Sigel, A. (Eds.), Metal Ions in Biological Systems, Mercury and its Effects on Environment and Biological Systems, vol. 34. Marcel Dekker Inc., New York, pp. 3–110.
Fitzgerald, W.F., Lamborg, C.H., 2003. Geochemistry of mercury in the environment. In: Lollar, B.S., Holland, H.D., Turekian, K.K. (Eds.), Treatise on Geochemistry. Elsevier, New York, pp. 107–148.
Frank, H., 1915. Contribución al conocimiento de las Salinas Grandes y la Mar Chiquita de la Provincia de Córdoba. Revista del Centro de Estudiantes de Ingienería 3, 91L 107.
Gagnon, C., Pelletier, É., Mucchi, A., 1997. Behaviour of anthropogenic mercury in coastal marine sediment. Marine Chemistry 59, 159–176.
Gaiero, D.M., Roman Ross, G., Depetris, P.J., Kempe, S., 1997. Spatial and temporal variability of total non-residual heavy metals content in stream sediments from the Suquía river system, Córdooba, Argentina. Water, Air and Soil Pollution 93, 303–319.
Gaiero, D.M., Brunet, F., Probst, J.-L., Depetris, P.J., 2007. A uniform isotopic and chemical signature of dust exported from Patagonia: rock sources and occurrence in southern environments. Chemical Geology 238 (1–2), 107–120.
Garreaud, R.D., Vuille, M., Compagnucci, R., Marengo, J., 2009. Present-day South American Climate (LOTRED South America). Palaeogeography, Palaeoclimatology, Palaeoecology 281, 180–195.
Gilli, A., Anselmetti, F.S., Ariztegui, D., 2005. Seismic stratigraphy, buried beach ridges and contourite drifts: the late quaternary history of the closed Lago Cardiel basin, Argentina (49°S). Sedimentology 51, 1–23.
Hermanns, Y.M., Biester, H., 2013. Anthropogenic mercury signals in lake sediments from southernmost Patagonia, Chile. Science of the Total Environment 445–446, 126–135.
Hudson-Edwards, K.A., Macklin, M.G., Miller, J.R., Lechler, P.J., 2001. Sources, distribution and storage of heavy metals in the Río Pilcomayo, Bolivia. Journal of Geochemical Exploration 72 (3), 229–250.
Huerta-Diaz, M.A., Morse, J.W., 1990. A quantitative method for determination of trace metal concentrations in sedimentary pyrite. Marine Chemistry 29, 119–144.
Huerta-Diaz, M.A., Morse, J.W., 1992. Pyritization of trace metals in anoxic marine sediments. Geochimica et Cosmochimica Acta 56 (7), 2681–2702.
Iriondo, M.H., 1989. Major fractures of the Chaco-Pampa plain. In: Mörner, N. (Ed.), Bullettin of the INQUA. Neotectonics Commission, NA, pp. 12–42.
Iriondo, M.H., 1997. Models of deposition of loess and loessoids in the Upper Quaternary of South America. Journal of South American Earth Sciences 10, 71–79.
Johannessen, S.C., Macdonald, R.W., Eek, K.M., 2005. Historical trends in mercury sedimentation and mixing in the strait of Georgia, Canada. Environmental Science and Technology 39, 4361–4368.
King, P., Kennedy, H., Newton, P.P., Jickells, T.D., Brand, T., Calvert, S., Cauwet, G., Etcheber, H., Head, B., Khripounoff, A., Manighetti, B., Miquel, J.C., 1998. Analysis of total and organic carbon and total nitrogen in settling oceanic particles and a marine sediment: an interlaboratory comparison. Marine Chemistry 60, 203–216.
Kostka, J.E., Luther III, G.W., 1994. Partitioning and speciation of solid phase iron in saltmarsh sediments. Geochimica et Cosmochimica Acta 58 (7), 1701–1710.
Kratzmann, D.J., Carey, S., Naranjo, J., 2008. Compositional variations and magma mixing in the 1991 eruptions of Hudson Volcano, Chile. Bulletin of Volcanology 71 (4), 419–439.
Kratzmann, D.J., Carey, S.N., Fero, J., Scasso, R.A., Naranjo, J.A., 2010. Simulations of tephra dispersal from the 1991 explosive eruptions of Hudson volcano Chile. Journal of Volcanology and Geothermal Research 190, 337–352.
Kröhling, D., Iriondo, M., 1999. Upper quaternary palaeoclimates of the Mar Chiquita area, North Pampa, Argentina. Quaternary International 57/58, 149–163.
Lacerda, L.D., De Souza, M., Ribeiro, M.G., 2004. The effects of land use change on mercury distribution in soils of Alta Floresta, Southern Amazon. Environmental Pollution 129, 247–255.
Lamborg, C.H., Fitzgerald, W.F., Damman, A.W.H., Benoit, J.M., Balcom, P.H., Engstrom, D.R., 2002. Modern and historic atmospheric mercury fluxes in both hemispheres: global and regional mercury cycling implications. Global Chemical Cycles 16 (4), 1104.
Langston, W.J., Burt, G.R., Pope, N.D., 1999. Bioavailability of metals in sediments of the Dogger Bank (central North Sea): a mesocosm study. Estuarine, Coastal and Shelf Science 48 (5), 519–540.
Larrose, A., Coynel, A., Schäfer, J., Blanc, G., Massé, L., Maneux, E., 2010. Assessing the current state of the Gironde Estuary by mapping priority contaminant distribution and risk potential in surface sediment. Applied Geochemistry 25, 1912–1923.
Liang, L., Sun, Y., Yao, Z., Liu, Z., Wu, F., 2012. Evaluation of high-resolution elemental analyses of Chinese loess deposits measured by X-ray fluorescence core scanner. Catena 92, 75–82.
Lofi, J., Weber, O., 2001. SCOPIX – digital processing of X-ray images for the enhancement of sedimentary structures in undisturbed core slabs. Geo Marine Letters 20, 182–186.
Löwemark, L., Chen, H.F., Yang, T.N., Kylander, M., Yu, E.F., Hsu, Y.W., Lee, T.Q., Song, S.R., Jarvis, S., 2011. Normalizing XRF-scanner data A cautionary note on the interpretation of high-resolution records from organic-rich lakes. Journal of Asian Earth Sciences 40, 1250–1256.
Ma, Y., Uren, N.C., 1995. Application of a new fractionation scheme for heavy metals in soils. Communications in Soil Science and Plant Analysis 26 (19–20), 3291–3303.
Marcovecchio, J.E., Andrade, S., Ferrer, L.D., Asteasuain, R.O., De Marco, S.G., Gavio, M.A., Scarlato, N., Freije, R.H., Pucci, A.E., 2001. Mercury distribution in estuarine environments from Argentina: the detoxification and recovery of salt marshes after 15 years. Wetlands Ecology and Management 9 (4), 317–322.
Markgraf, V., 1998. Past climate of South America. In: Hobbs, J.E., Lindesay, J.A., Bridgman, H.A. (Eds.), Climate of the Southern Continents: Present, Past and Future. John Wiley & Sons Ltd., Hoboken, NJ.
Martínez, D.E., 1991. Caracterización geoquímica de las aguas de la Laguna Mar Chiquita Provincia de Córdoba. Universidad Nacional de Córdoba – Facultad de Ciencias Exactas Físicas y Naturales, pp. 284 (Doctoral Thesis).
Martínez, D.E., Gómez Peral, M.A., Maggi, J., 1994. Caracterización geoquímica y sedimentológica de los fangos de la laguna Mar Chiquita, Provincia de Córdoba: aplicación del análisis multivariante. Revista de la Asociación Geológica Argentina 49 (1–2), 25–38.
Matthews, S.J., Gardeweg, M.C., Sparks, R.S.J., 1997. The 1984 to 1996 cyclic activity of Láscar Volcano, northern Chile: cycles of dome growth, dome subsidence, degassing and explosive eruptions. Bulletin of Volcanology 59 (1), 72–82.
Migeon, S., Weber, O., Faugeres, J.-C., Saint-Paul, J., 1999. SCOPIX A new imaging system for core analysis. Geo-Marine Letters 18, 251–255.
Mon, R., Gutiérrez, A., 2009. The Mar Chiquita Lake: an indicator of intraplate deformation in the central plain of Argentina. Geomorphology 111, 111–122.
Monferrán, M.V., Galanti, L.N., Bonansea, R.I., Amé, M.V., Wunderlin, D.A., 2011. Integrated survey of water pollution in the Suquía River basin (Córdoba, Argentina). Journal of Environmental Monitoring 13, 398–409.
Montero-Serrano, J.C., Bout-Roumazeilles, V., Sionneau, T., Tribovillard, N., Bory, A., Flower, B.P., Riboulleau, A., Martinez, P., Billy, I., 2010. Changes in precipitation regimes over North America during the Holocene as recorded by mineralogy and geochemistry of Gulf of Mexico sediments. Global and Planetary Change 74, 132–143.
Moreno, A., Giralt, S., Valero-Garcés, B., Sáez, A., Bao, R., Prego, R., Pueyo, J.J., González-Sampériz, P., Taberner, C., 2007. A 14 kyr record of the tropical Andes: the Lago Chungara sequence, 18 S, northern Chilean Altiplano. Quaternary International 161, 4–21.
Nova-López, C., Huerta-Díaz, M.A., 2001. Degree of trace metal pyritization in sediments from the Pacific coast of Baja California, Mexico. Ciencias Marinas 27 (2), 289–309.
Olivero, J., Johnson, B., Arguello, E., 2002. Human exposure to mercury in San Jorge river basin Colombia (South America). The Science of the Total Environment 289, 41–47.
Osores, M.S., Pujol, G., Collini, E., Folch, A., 2011. Análisis de la dispersión y depósito de ceniza volcánica mediante el modelo fall3d para la erupción del volcán Hudson en 1991. Trabajo para el Servicio de Hidrografía Naval y el Servicio Meteorológico Nacional.
Pasquini, A.I., Lecomte, K.L., Piovano, E.L., Depetris, P.J., 2006. Recent rainfall and runoff variability in central Argentina. Quaternary International 158, 127–139.
Pasquini, A.I., Formica, S.M., Sacchi, G.A., 2011. Hydrochemistry and nutrients dynamic in the Suquía River urban catchment's, Córdoba, Argentina. Environmental Earth Science, http://dx.doi.org/10.1007/s12665-011-0978-z.
Pesce, S.F., Wunderlin, D.A., 2000. Use of water quality indices to verify the impact of Córdoba City Argentina, on Suquía River. Water Research 34 (11), 2915–2926.
Piovano, E.L., Ariztegui, D., Damatto Moreira, S., 2002. Recent environmental changes in Laguna Mar Chiquita (central Argentina): a sedimentary model for a highly variable saline lake. Sedimentology 49, 1371–1384.
Piovano, E.L., Ariztegui, D., Bernasconi, S.M., McKenzie, J.A., 2004a. Stable isotopic record of hydrological changes in subtropical Laguna Mar Chiquita (Argentina) over the last 230 years. The Holocene 14 (4), 525–535.

Piovano, E.L., Larizzatti, F.E., Fávaro, D.I., Oliveira, S.M.B., Damatto, S.R., Mazzilli, B.P., Ariztegui, D., 2004b. Geochemical response of a closed-lake basin to 20th century recurring droughts/wet intervals in the subtropical Pampean Plains of South America. Journal of Limnology 63 (1), 21–32.

Piovano, E.L., Ariztegui, D., Córdoba, F., Cioccale, M., Sylvestre, F., 2009. Hydrological variability in South America below the Tropic of Capricorn (Pampas and Patagonia, Argentina) During the Last 13.0 Ka. In: Vimeux, F., Sylvestre, F., Khodri, M. (Eds.), Past Climate Variability in South America and Surrounding Regions, From the Last Glacial Maximum to the Holocene, vol. 14. Springer, pp. 323–351.

Quevauviller, P., 1998. Method Performance Studies for Speciation Analysis. Royal Society of Chemistry, Cambridge, UK.

Quintana, E., 2011. Environmental impact of the nuclear tests in Argentina. In: Comprehensive Nuclear-Test-Ban Treaty, Science and Technology, Vienna, Austria, 8–10 June 2011.

Raiswel, R., Canfield, D.E., Berner, R.A., 1994. A comparison of iron extraction methods for the determination of degree of pyritization and the recognition of iron-limited pyrite formation. Chemical Geology 111 (1–4), 101–110.

Reati, G.J., Florín, M., Fernández, G.J., Montes, C., 1997. The Laguna Mar Chiquita (Córdoba, Argentina): a little known, secularly fluctuating, saline lake. International Journal of Salt Lake Research 5, 187–219.

Ribeiro Guevara, S., Massaferro, J., Villarosa, G., Arribére, M., Rizzo, A., 2002. Heavy metal contamination in sediments of lake Nahuel Huapi, Nahuel Huapi National Park, Northern Patagonia, Argentina. Water, Air, and Soil Pollution 137 (1–4), 21–44.

Ribeiro Guevara, S., Rizzo, A., Sánchez, R., Arribére, M., 2005. Heavy metal inputs in Northern Patagonia lakes from short sediment core analysis. Journal of Radioanalytical and Nuclear Chemistry 265 (3), 481–493.

Ribeiro Guevara, S., Catán, S.P., Marvin-Di Pasquale, M., 2009. Benthic methylmercury production in lacustrine ecosystems of Nahuel Huapi National Park, Patagonia, Argentina. Chemosphere 77 (4), 471–477.

Ribeiro Guevara, S., Meili, M., Rizzo, A., Daga, R., Arribére, M., 2010. Sediment records of highly variable mercury inputs to mountain lakes in Patagonia during the past millennium. Atmospheric Chemistry and Physics 10, 3443–3453.

Robbins, J.A., Edgington, D.N., 1975. Determination of recent sedimentation rates in Lake Michigan. Geochimica et Cosmichimica Acta 39, 285–304.

Rodrigues Bastos, W., Oliveira Gomes, J.P., Cavalcante Oliveira, R., Almeida, R., Nascimento, E.L., Bernardi, J.V.E., Drude de Lacerda, L., da Silveira, E.G., Pfeiffer, W.C., 2006. Mercury in the environment and riverside population in the Madeira River Basin Amazon, Brazil. Science of the Total Environment 368, 344–351.

Ronco, A., Camilión, C., Manassero, M., 2001. Geochemistry of heavy metals in bottom sediments from streams of the western coast of the Rio de la Plata Estuary, Argentina. Environmental Geochemistry and Health 23 (2), 89–103.

Rosenberg, E., Ariese, F., 2001. Quality control in speciation analysis. In: Ebdon, L., Pitts, L., Cornelis, R., Crews, H., Donard, O.F.X., Quevauviller Ph (Eds.), Trace Element Speciation for Environment, Food and Health, 2001. The Royal Society of Chemistry, Cambridge, UK, pp. 17–50 (Chapter 7).

Rothwell, R.G., Rack, F.R., 2006. New techniques in sediment core analysis: an introduction. In: Rothwell, R.G. (Ed.), New Techniques in Sediment Core Analysis. Special Publications. Geological Society, London, pp. 1–29.

Saari, H.-K., Schmidt, S., Castaing, P., Blanc, G., Sautour, B., Masson, O., Kirk Cochran, J., 2010. The particulate 7Be/210Pbxs and 234Th/210Pbxs activity ratios as tracers for tidal-to-seasonal particle dynamics in the Gironde estuary (France): implications for the budget of particle-associated contaminants. Science of the Total Environment 408, 4784–4794.

Sahuquillo, A., Rauret, G., Bianchi, M., Rehnert, A., Muntau, H., 2003. Mercury determination in solid phases from application of the modified BCR-sequential extraction procedure: a valuable tool for assessing its mobility in sediments. Analytical and Bioanalytical Chemistry 375 (4), 578–583.

Sanchez-Cabeza, J.A., Ruiz-Fernández, A.C., 2012. ^{210}Pb sediment radiochronology: an integrated formulation and classification of dating models. Geochimica et Cosmochimica Acta 82, 183–200.

Schäfer, J., Blanc, G., Audry, S., Cossa, D., Bossy, C., 2006. Mercury in the Lot-Garonne River system (France): sources fluxes and anthropogenic component. Applied Geochemistry 21, 515–527.

Schmidt, S., Howa, H., Mouret, A., Lombard, F., Anschutz, P., Labeyrie, L., 2009. Particle fluxes and recent sediment accumulation on the Aquitanian margin of Bay of Biscay. Continental Shelf Research 29, 1044–1052.

Selin, N., 2009. Global biogeochemical cycling of mercury: a review. Annual Review of Environment and Resources 34, 43–63.

Silvestri, G., 2004. El Niño signal variability in the precipitation over southeastern South America during the austral summer. Geophysical Research Letters 31, L18206.

Streets, D.G., Hao, J., Wu, Y., Jiang, J., Chan, M., Tian, H., Feng, X., 2005. Anthropogenic mercury emissions in China. Atmospheric Environment 39, 7789–7806.

Tack, F.M.G., Vossius, H.A.H., Verloo, M.G., 1996. A comparison between sediment fractions, obtained from sequential extraction and estimated from single extractions. International Journal of Environmental Analytical Chemistry 63 (1), 61–66.

Tessier, A., Campbell, P.G.C., Bisson, M., 1979. Sequential extraction procedure for the speciation of particulate trace metals. Analytical Chemistry 51 (7), 844–851.

Tjallingii, R., Röhl, U., Kölling, M., Bickert, T., 2007. Influence of the water content on X-ray fluorescence core-scanning measurements in soft marine sediments. Geochemistry, Geophysics, Geosystems 8 (2), http://dx.doi.org/10.1029/2006GC001393.

Troin, M., Vallet-Coulomb, C., Sylvestre, F., Piovano, E., 2010. Hydrological modelling of a closed lake (Laguna Mar Chiquita, Argentina) in the context of 20th century climatic changes. Journal of Hydrology 393, 233–244.

UNSCEAR, 2000. United Nations, New York, 654 pp.

Van der Klooster, E., van Egmond, F.M., Sonneveld, M.P.W., 2011. Maping soil clay contents in Dutch marine districts using gamma-ray spectrometry. European Journal of Soil Science 62, 743–753.

Von Guten, H.R., Strum, M., Moser, R.N., 1997. 200-year record of metals in Lake sediments and natural backgrounds concentration. Environmental Science and Technology 31, 2193–2197.

Weltje, G.J., Tjallingii, R., 2008. Calibration of XRF core scanners for quantitative geochemical logging of sediment cores: theory and application. Earth and Planetary Science Letters 274, 423–438.

Wilson, T.M., Cole, J.W., Stewart, C., Croning, S.J., Johnston, D.M., 2011. Ash storms. Impacts of wind-remobilised volcanic ash on rural communities and agriculture following the 1991 Hudson eruption, southern Patagonia, Chile. Bulletin of Vulcanology 73, 223–239.

Wunderlin, D.A., Díaz, M.P., Amé, M.V., Pesce, S.F., Hued, A.C., Bistoni, M.A., 2001. Pattern recognition techniques for the evaluation of spatial and temporal variations in water quality. A case study: Suquía River Basin (Córboba-Argentina). Water Resources 12, 2881–2894.

Zárate, M., 2003. Loess of Southern America. Quaternary Science Reviews 22, 1987–2006.